APPLIED GEOPHYSICS, Vol.12, No.2 (June 2015), P. 137-146, 6 Figures.
DOI:10.1007/s11770-015-0491-2

3D density inversion of gravity gradient data using the extrapolated Tikhonov regularization*

Liu Jin-Zhao[1,2♦], Liu Lin-Tao[2], Liang Xing-Hui[2], and Ye Zhou-Run[2]

Abstract: We use the extrapolated Tikhonov regularization to deal with the ill-posed problem of 3D density inversion of gravity gradient data. The use of regularization parameters in the proposed method reduces the deviations between calculated and observed data. We also use the depth weighting function based on the eigenvector of gravity gradient tensor to eliminate undesired effects owing to the fast attenuation of the position function. Model data suggest that the extrapolated Tikhonov regularization in conjunction with the depth weighting function can effectively recover the 3D distribution of density anomalies. We conduct density inversion of gravity gradient data from the Australia Kauring test site and compare the inversion results with the published research results. The proposed inversion method can be used to obtain the 3D density distribution of underground anomalies.
Keywords: extrapolated Tikhonov regularization, depth weighting, gravity gradient tensor, eigenvector

Introduction

Gravity gradiometry in hydrocarbon and mineral exploration is behind many processing and interpretation methods of potential field data (Pawlowski, 1998; Lee, 2001; Dransfield, 2007), especially, 3D inversion of magnetic and gravitational data. For example, Ke et al. (2009) used damped least squares in 3D gravity density inversion. Feng et al. (2014) used forward modeling and inversion to study density interfaces and gravity anomalies, respectively. Liu (2013) and Wang et al. (2014) extrapolated the Tikhonov regularization to the density-constrained 3D inversion of gravity data. Bear et al. (1995) used an improved Levenburg–Marquart algorithm in order to invert Bouguer gravity data to obtain the 3D density distribution. Li and Oldenburg et al. (1996, 1998) applied the depth weighting function to surface magnetic or gravity data inversion and recovered the 3D distribution of the density contrast. Rama et al. (1999) proposed an inversion scheme to trace 3D density interfaces using gravity grids. Zhdanov et al. (2002) conducted 3D density inversion of gravity data based on the focusing inversion method and obtained good results. Compared with conventional inversion of gravity data, however, inversion of high spatial resolution gravity gradient tensor data can better establish the boundaries of underground anomalies and recover the 3D density

Manuscript received by the Editor August 2, 2014; revised manuscript received February 18, 2015.
*This work is supported by National major special equipment development (No. 2011YQ120045) and The National Natural Science Fund (No. 41074050 and 41304023).
1. First Crust Monitoring and Application Center, China Earthquake Administration, Tianjin 300180, China.
2. State Key Laboratory of Geodesy and Earth's Dynamics, Institute of Geodesy and Geophysics, CAS, Wuhan, 430077, China.
♦Corresponding Author: Liu Jin-Zhao (Email: whiggliujinzhao@126.com)

distribution. This has been widely used in delineating hydrocarbon deposits and geological structures; gravity gradient tensor data can be used in 3D inversion to map the subtleties of geological anomalies. For example, Wang et al. (2013) applied 3D density inversion to gravity gradient data and constrained the inversion process by using the projected gradient algorithm. Guo et al. (2011) and Chen et al. (2013) applied 3D density inversion to tensor gravity gradient data based on the quasi back-propagation (BP) neural network algorithm and the preconditioned conjugate gradient algorithm. Li (2001) introduced an inversion algorithm for multicomponent gravity gradiometry data to recover the 3D density contrast in salt dome imaging. Zhdanov et al. (2004) developed a method based on the regularized focusing inversion to interpret components of the tensor gravity gradient and showed via numerical modeling and inversion that the focusing inversion can obtain sharper images of geological targets when compared with conventional maximum smoothness inversion. Vasilevsky et al. (2005) proposed the regularized inversion of full tensor gravity gradient data for the dynamic monitoring of hydrocarbon reservoirs. In addition, Guo et al. (2009) proposed the 3D correlation imaging of gravity anomaly and gravity gradiometry data. Routh et al. (2001) presented two methods for inverting the base of the salt interface using surface gravity and tensor gravity data.

Variable underground density distributions can produce similar gravity fields. In surveying, the inversion of potential field data is often ill posed when prior information of the regional geology is insufficient. Ill-posed matrix inversion produces weak perturbations in observations that seriously affect the inversion results. Tikhonov regularization is often used to obtain stable approximate solutions. Nevertheless, attention should be paid on selecting and using the regularization parameters because they can introduce errors to the approximate solutions (Tikhonov and Arsenin, 1977). Hämarik et al. (2007, 2008) proposed the extrapolated Tikhonov regularization to minimize the deviations between observed and calculated data, and obtained the best results by linearly combining the inversion solutions.

In 3D density inversion of potential field data, the attenuation of the position function increases with depth. To address this issue, many researchers have proposed different depth weighting functions for gravity and magnetic data inversion. Most of the depth weighting functions, however, are used to stabilize the boundary constraints functional in model objective function. In this study, we present a modified depth weighting function that requires less prior information and is easier to apply to the misfit functional (see also Commer, 2011). The modified depth weighting function is derived from the gravity gradient eigenvector rather than prior information (Beiki and Pedersen, 2010; Wedge, 2013). Inversion of model data suggests that the method can eliminate inaccuracies in the density distribution caused by excessive near-surface weighting and improves the inversion distribution. Finally, we apply 3D density inversion to gravity gradient data from the Australia Kauring airborne gravimetry test site and compare the results with published research results. Thus, we verify that the extrapolated Tikhonov regularization in conjunction with the gravity gradient eigenvector depth weighting function can be used in 3D density inversion.

Methodology

Inversion theory

For any underground geological body with known density distribution, the gravity gradient tensor in the local Cartesian coordinate system can be expressed as

$$\Gamma = \Delta U = \begin{bmatrix} \frac{\partial^2 U}{\partial x_1^2} & \frac{\partial^2 U}{\partial x_1 \partial x_2} & \frac{\partial^2 U}{\partial x_1 \partial x_3} \\ \frac{\partial^2 U}{\partial x_2 \partial x_1} & \frac{\partial^2 U}{\partial x_2^2} & \frac{\partial^2 U}{\partial x_2 \partial x_3} \\ \frac{\partial^2 U}{\partial x_3 \partial x_1} & \frac{\partial^2 U}{\partial x_3 \partial x_2} & \frac{\partial^2 U}{\partial x_3^2} \end{bmatrix} = \begin{bmatrix} \Gamma_{11} & \Gamma_{12} & \Gamma_{13} \\ \Gamma_{21} & \Gamma_{22} & \Gamma_{23} \\ \Gamma_{31} & \Gamma_{32} & \Gamma_{33} \end{bmatrix}, \quad (1)$$

where Γ is the gravity gradient tensor, U is the gravitational potential, x_1, x_2, and x_3 represent three mutually orthogonal axes in the direction of the Cartesian coordinate system, and Γ_{ij} (i, j = 1, 2, 3) represent the individual components of the gravity gradient tensor.

Outside the source, the gravitational potential U satisfies the Laplace equation $\Gamma_{11} + \Gamma_{22} + \Gamma_{33} = 0$ and, owing to the symmetry $\Gamma_{ij} = \Gamma_{ji}$ (i, j = 1, 2, 3), there are only five independent components in the nine components of the gravity gradient full tensor.

In 3D density inversion, we divide the underground space into closely arranged cubic cells, referred to as prisms in this study, with constant density contrast. We select only inversion solutions that agree with the observed data. First, we calculate the gravity gradient tensor of each observation at the Earth's surface

according to the equation

$$\Gamma_{ij}^{\ n} = \sum_{m=1}^{M} a_{nm}\rho_m,$$
$$(i,j=1,2,3;\ m=1,2,...,M;n=1,2,...,N), \qquad (2)$$

where $\Gamma_{i,j}^{n}$ is the gravity gradient at observation point n for N observations, ρ_m is the density contrast of the mth cell, referred to as prism in this study, and there are M cells, and a_{nm} is the position function of the gravity gradient tensor of the mth cell at observation point n.

For multicomponent gravity gradient data, the total number of observations is $S = N \times p$, where p is the number of gravity gradient components. The matrix of the multicomponent gravity gradient is

$$\underset{S\times 1}{\mathrm{d}} = \underset{S\times M}{\mathrm{A}} \times \underset{M\times 1}{\mathrm{m}}, \qquad (3)$$

where A is the position function matrix and $m = [\rho_1, \rho_2, \rho_M]^{\mathrm{T}}$ is the parameter matrix to be inverted.

Because the position function matrix A is often ill conditioned, equation (3) is consequently ill posed. This implies that the computed solution is potentially very sensitive to perturbations in the left-hand side of equation (3). However, stable solutions can be obtained with the Tikhonov regularization algorithm, which is the most common and well-known regularization method. Stable approximate solutions can be obtained with the Tikhonov regularization algorithm by minimizing the misfit norm and the norm of the boundary constraints

$$\underset{M\times 1}{\mathrm{m}}_{\alpha}^{\mathrm{T}} = \arg\min\left[\left\|\underset{S\times M}{\mathrm{A}}\ \underset{M\times 1}{\mathrm{m}} - \underset{S\times 1}{\mathrm{d}}\right\|_2^2 + \alpha\left\|\underset{S\times M}{\mathrm{L}}\left(\underset{M\times 1}{\mathrm{m}} - \underset{M\times 1}{\mathrm{m}^*}\right)\right\|_2^2\right], \quad (4)$$

where argmin denotes the minimization of the objective function. The regularization parameter α controls the weight allocation between the minimization misfit and boundary constraints norms. Matrix L is typically either the identity matrix or an $S \times M$ discrete approximation differential operator. m* is the prior estimation of the inversion density vector. m_{α}^{T} is the regularization solution that corresponds to the regularization parameter α.

Although the introduction of regularization parameters in the Tikhonov regularization can yield stable approximate solutions, it also introduces errors. Assuming that the potential field data contain noise and the noise level satisfies $||\mathrm{Am-d}||^2 \le \delta$, where δ is the error criterion defined by the interpreter. To reduce the inversion errors caused by the introduction of the regularization parameters, Hämarik (2007) proposed a new algorithm for obtaining the desired solutions by linearly combining the approximate inversion solutions that correspond to the different regularization parameters using the Lagrange interpolation method, which is known as the extrapolated Tikhonov regularization.

We define $\mathrm{m}_{\alpha i}$ as the regularization solution sequence according to the different regularization parameters α_i ($\alpha_{i-1} = \alpha_i/q$), where $i = 1, 2, \ldots, k$ and q is a proportional constant used to produce the regularization parameters, to control the convergence speed. Thus, the approximate solutions derived with the extrapolated Tikhonov regularization are expressed as

$$\mathrm{m}_{\alpha_1,\alpha_2,...,\alpha_k}^{\mathrm{ET}} = \sum_{i=1}^{k} d_i \mathrm{m}_{\alpha_i} = \sum_{i=1}^{k}\prod_{j=1,j\neq i}^{k}\left(1-\frac{\alpha_i}{\alpha_j}\right)^{-1}\mathrm{m}_{\alpha_i}. \quad (5)$$

Note that the choice of α_i and k directly affects the ill-conditioned linear inversion or the degree of approximation between inversion and theoretical solutions. We select parameters α_i and k based on the monotone error rule. For other parameter selection rules, such as the discrepancy principle, balancing principle, and rules R1 and R2, the reader can refer to Palm (2010).

Modified depth weighting function

In 3D density inversion of gravity or gravity gradient data, the position function attenuation increases with depth, which affects the distribution of the inverted density at the surface and causes deviations from the real underground anomaly density distribution. Many have studied the depth weighting function and most studies have focused on the decaying resolution with depth ((Li and Oldenbrug, 1998; Zhdanov, 200s). These methods basically operate on the boundary constraints functional (Li and Oldenbrug, 1998; Zhdanov, 2002). Using gravity gradient data and the depth weighting function of Commer (2011), we propose a modified depth weighting function based on the gravity gradient eigenvector that directly acts on the misfit function

$$f(z) = \frac{\mu + \exp\left[\frac{\kappa}{D}\left(z - mc(C_{\max}^{voxel})\right)\right]}{1 + \exp\left[\frac{\kappa}{D}\left(z - mc(C_{\max}^{voxel})\right)\right]}, \qquad (6)$$

where μ is an empirical parameter, which Commer (2011) suggested it is equal to 0.001, κ is the scaling factor that controls $f(z) \approx \mu$ when $z = 0$, and D is the depth of the inversion density space and is generally 2–3 times the depth of the mass center of the anomaly. In this study, we use $\mu = 0.01$, $\kappa = 10$, $D = 500$, and take $mc\left(C_{\max}^{voxel}\right)$ to represent the depth of the mass center of the anomaly. In equation (6), it is crucial to determine $mc\left(C_{\max}^{voxel}\right)$.

Commer (2011) set $mc\left(C_{\max}^{voxel}\right) = z_c = (z_1 + z_2)/2$, where z_1 and z_2 are the upper and lower cube boundaries, respectively. However, z_1 and z_2 are often unknown; therefore, we have to calculate $mc\left(C_{\max}^{voxel}\right)$.

According to Beiki and Pedersen (2010), if λ_1 is the principle eigenvector of the gravity gradient tensor of an observation point, the corresponding eigenvector p_1 is parallel to the line direction defined by observation point x and the mass center x^{mc} of the anomaly

$$p_1 = \left(x_1^{mc} - x_1, x_2^{mc} - x_2, x_3^{mc} - x_3\right) / R, \qquad (7)$$

where $R = \sqrt{(x_1\ m^c - x_1)^2 + (x_2\ m^c - x_2)^2 + (x_3\ m^c - x_3)^2}$ is the distance between observation x and mass center x^{mc} of the anomaly. The underground inversion space can be divided into closely arranged body elements. We consider that the line defined by the eigenvector corresponding to the principle eigenvalue of the gravity gradient tensor at each observation point must penetrate through each element in the elements array. Then, the value of the penetrated element is estimated and this process is repeated until all observation points are involved in the calculation. The location of the element with the largest value denotes the mass center of the subsurface anomaly; thus, the depth of the subsurface anomaly is also obtained. The value of all observations that penetrate through each element within the inversion space is

$$C_k^{voxel} = \sum_{n=1}^{N} w_n^k c_n^k, k = 1, 2, ..., M, \qquad (8)$$

M and N are the number of prisms and number of observations, respectively. C_k^{voxel} is the cumulative value of prism k, c_n^k is the single value of prism k projected onto the observation point n, and w_n^k is the weighting function.

By comparing the cumulative value of the different discrete prisms, the depth of the cubic cell with the largest amplitude is the depth of the mass center of the anomaly $mc(C_k^{voxel})$. Then, the grid value of the depth weighting function $f(z)$ is directly applied to the position function matrix A in equation (5) and by using the extrapolated Tikhonov regularization we can obtain the inversion solution (Liu, 2013).

Inversion parameter constraints

Commer (2001) constrained the inversion parameters to obtain geologically meaningful inversion solutions. We also apply constraints to the inversion parameters of 3D gravity gradient density data with the following equation

$$x = \frac{a + b\exp(pm)}{1 + \exp(pm)}, \quad -\infty < m < \infty. \qquad (9)$$

where a and b are the lower and upper bounds, and parameter p controls the transfer efficiency of m near 0 in the transformed space. Liu (2013) suggested that parameter p should be between 1.2 and 1.4 to obtain meaningful inversion solutions. m and x are density vectors before and after the application of the constraints.

Theoretical examples

To test the proposed 3D inversion method, we considered two rectangular prisms at 100 m depth, with same dimensions of 200 m × 200 m × 200 m and density of 1000 kg/m^3. The locations of the prisms are shown in Figures 1a–1c. The background density is 0 kg/m^3. The gravity gradient of the models at the Earth's surface can be calculated with the following equations

$$\Gamma_{ij}(x) = G\rho\iint_{\sigma}\int_{0}^{h(x_1', x_2')} F_{ij}\, dx_3' d\sigma = G\rho\iint_{\sigma} R_{ij}\, d\sigma = \rho\sum_{m=1}^{M} G R_{ij}\, d\sigma, \qquad (10)$$

$$R_{11} = \begin{cases} -\dfrac{1}{2(x_3 - x_3')^2}\Big|_{x_3'=0}^{h}, s = 0 \\ \dfrac{1}{s^4}\left((s^2 - 3(x_1 - x_1')^2)\dfrac{(x_3 - x_3')}{r} + \dfrac{(x_1 - x_1')^2(x_3 - x_3')}{r^3}\right)\Big|_{x_3'=0}^{h}, s \neq 0 \end{cases}, \qquad (11)$$

$$R_{12} = \begin{cases} 0, s = 0 \\ \dfrac{(x_1 - x_1')(x_2 - x_2')}{s^4}\left(\dfrac{(x_3 - x_3')^3}{r^3} - \dfrac{3(x_3 - x_3')}{r}\right)\Big|_{x_3'=0}^{h}, s \neq 0 \end{cases}, \qquad (12)$$

$$R_{13} = \frac{x_1 - x_1^{'}}{r^3}\Big|_{x_3^{'}=0}^{h}, \tag{13}$$

$$R_{22} = \begin{cases} -\dfrac{1}{2(x_3 - x_3^{'})^2}\Big|_{x_3^{'}=0}^{h}, s = 0 \\ \dfrac{1}{s^4}\left((s^2 - 3(x_2 - x_2^{'})^2)\dfrac{(x_3 - x_3^{'})}{r} + \dfrac{(x_2 - x_2^{'})^2 (x_3 - x_3^{'})}{r^3} \right)\Big|_{x_3^{'}=0}^{h}, s \neq 0 \end{cases}, \tag{14}$$

$$R_{23} = \frac{x_2 - x_2^{'}}{r^3}\Big|_{x_3^{'}=0}^{h}, \tag{15}$$

$$R_{33} = \frac{x_3 - x_3^{'}}{r^3}\Big|_{x_3^{'}=0}^{h}, \tag{16}$$

where $i, j = 1, 2, 3$, G is the gravitational constant, ρ is the density contrast of the surrounding rocks, and r and s are the space and plane distances between observations and integral points.

We divide the underground space into closely arranged prisms; the dimensions of cubes with constant unit density is 50 m ×50 m × 50 m. Therefore, the total number of prisms in the underground space is 4000, as shown in Figure 1. Using the six components of the gravity gradient tensor Γ_{11}, Γ_{12}, Γ_{13}, Γ_{22}, Γ_{23}, and Γ_{33}, the Tikhonov regularization, and the extrapolated Tikhonov regularization, we calculate the inversion density vectors of the underground space and list the fitting error norm in Table 1.

Table 1 Fitting error norm derived with the two regularization methods and different error levels

Error level	10^{-1}	10^{-2}	10^{-3}	10^{-4}	
T	0.0783	0.0037	6.1308×10^{-4}	8.6418×10^{-5}	$q = 2$
ET	0.0312	0.0033	4.9696×10^{-4}	2.8982×10^{-5}	
T	0.0783	0.0083	8.6589×10^{-4}	8.6418×10^{-5}	$q = 2^{0.75}$
ET	0.0524	0.0057	3.9800×10^{-4}	2.9037×10^{-5}	
T	0.0783	0.0063	8.6589×10^{-4}	8.6418×10^{-5}	$q = 2^{0.5}$
ET	0.0528	0.0021	3.5996×10^{-4}	3.7534×10^{-5}	
T	0.0960	0.0083	8.6589×10^{-4}	8.6418×10^{-5}	$q = 2^{0.25}$
ET	0.0415	0.0034	4.5022×10^{-4}	4.8601×10^{-5}	

Note: T denotes the Tikhonov regularization algorithm and ET denotes the extrapolated Tikhonov regularization algorithm.

The fitting error norm $||\mathrm{Am\text{-}d}||^2$ calculated by using the Tikhonov regularization and extrapolated Tikhonov regularization algorithms at different error levels ($\delta = 10^{-1}$, $\delta = 10^{-2}$, $\delta = 10^{-3}$, and $\delta = 10^{-4}$) and different proportional constants of the regularization parameters ($q = 2$, $q = 20.75$, $q = 20.5$, and $q = 20.25$) are given in Table 1. We can see that the precision of the inversion with the extrapolated Tikhonov regularization algorithm is better; thus, we only discuss the 3D density inversion derived with the extrapolated Tikhonov regularization algorithm in the example below.

We select a sequence of regularization parameters α_i, $i = 1, 2, \ldots, N$ for solving the ill-posed problem of 3D density inversion using the extrapolated Tikhonov regularization algorithm. We set the initial N equal to 500 and use the following proportional coefficients 2, $2^{0.75}$, $2^{0.5}$, and $2^{0.25}$ to control the convergence speed of the sequence of regularization parameters. δ is the error criterion defined by the interpreter.

According to equation (5), the linear combination of the different regularization solutions corresponds to the different regularization parameters α_i. k and α_k are the two regularization parameters in the sequence of regularization parameters that satisfy the prior error level and are chosen by using different selection rules. We use the monotone error rule in selecting the parameters. For a given regularization parameter sequence $\alpha_1 \geq \alpha_2 \geq \ldots$, we denote $\mathrm{m}_n = \mathrm{m}_{\alpha 1, \alpha 2, \ldots, \alpha n}$, $\mathrm{r}_n = \mathrm{Am}_n - \mathrm{d}$, and $D_{\mathrm{ME}}(n) =$

$(r_n + r_{n+1}, r_{n+1})/(2||r_{n+1}||)$. Then, we assign n that satisfies $D_{ME}(n) \leq \delta$ and k to the total number of extrapolating items in the extrapolated Tikhonov algorithm and the regularization parameter α_k. For more parameter selection rules, the reader can refer to the literature.

Finally, we obtain the results by using the extrapolated Tikhonov regularization algorithm in conjunction with the modified depth weighting function based on the gravity gradient eigenvector and the inversion constraint function (Figure 1). Figures 1a–1c show the vertical section, top transverse section, and bottom transverse section of the prism model, respectively, where the distance between the top surface of the prisms and the Earth's surface is 100 m. Figures 1d–1f show the vertical section, the top transverse section, and bottom transverse section of the inverse solutions derived with the extrapolated Tikhonov regularization algorithm before applying the depth weighting and parameter constraints. Figures 1g–1i show the vertical section, top transverse section, and bottom transverse section of the inversion solutions derived with the extrapolated Tikhonov regularization algorithm after applying the depth weighting and parameter constraints.

From Figure 1, we see that the inversion solutions derived with the extrapolated Tikhonov regularization algorithm agree with the top part of the model (Figures

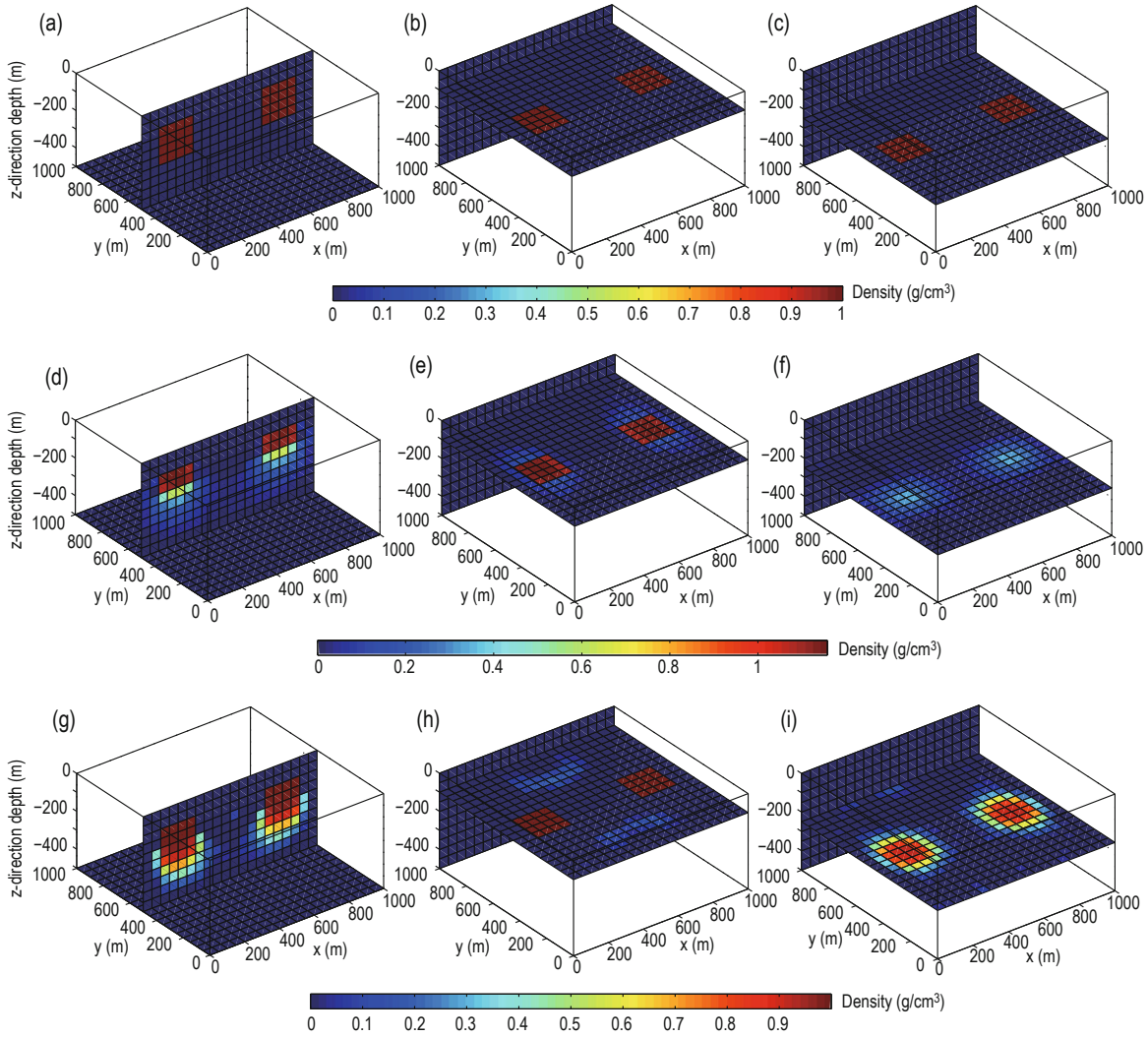

Fig.1 Inversion results with the extrapolated Tikhonov regularization algorithm before and after the application of depth weighting and parameter constraints.

(a)−(c) vertical section, top transverse section, and bottom transverse section of the synthetic prism models; the distance between the top surface of the prism model and the ground surface is 100 m; (d)−(f) inversion results of the extrapolated Tikhonov regularization algorithm before applying depth weighting and parameter constraints; (g)−(i) inversion results of the extrapolated Tikhonov regularization algorithm after applying depth weighting and parameter constraints.

1b and 1e). Prior to depth weighting, the inversion solutions did not match with the bottom part of the model owing to the fast attenuation of the kernel function with increasing depth. Thus, we use the modified depth weighting function to address this issue and show the results in Figure 2.

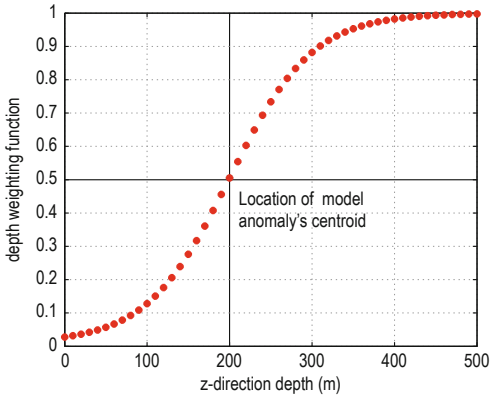

Fig. 2 Depth weighting function vs depth.

The results for the location of the mass center of the model density anomaly are shown in Figure 3, in which we have calculated the cumulative value of the six transverse sections. The depths are −50 m, −100 m, −150 m, −200 m, −250 m, and −300 m, respectively, and we find that the largest cumulative value is in the transverse section with depth −200 m (Figure 3d). This means that the mass center of the model density anomaly is 200 m from the ground surface. Based on the detected depth of the mass center, we calculate the inversion solutions after applying depth weighting and show the results in Figures 1g–1i. We find that the depth weighing function partially offsets the undesired effects to the density distribution caused by the kernel function attenuation. In terms of the distribution of the inversion densities at the bottom of the anomaly, the solutions after depth weighting are better than those prior to depth weighting; however, the distribution of the inversion densities somewhat diverges at the bottom of the model.

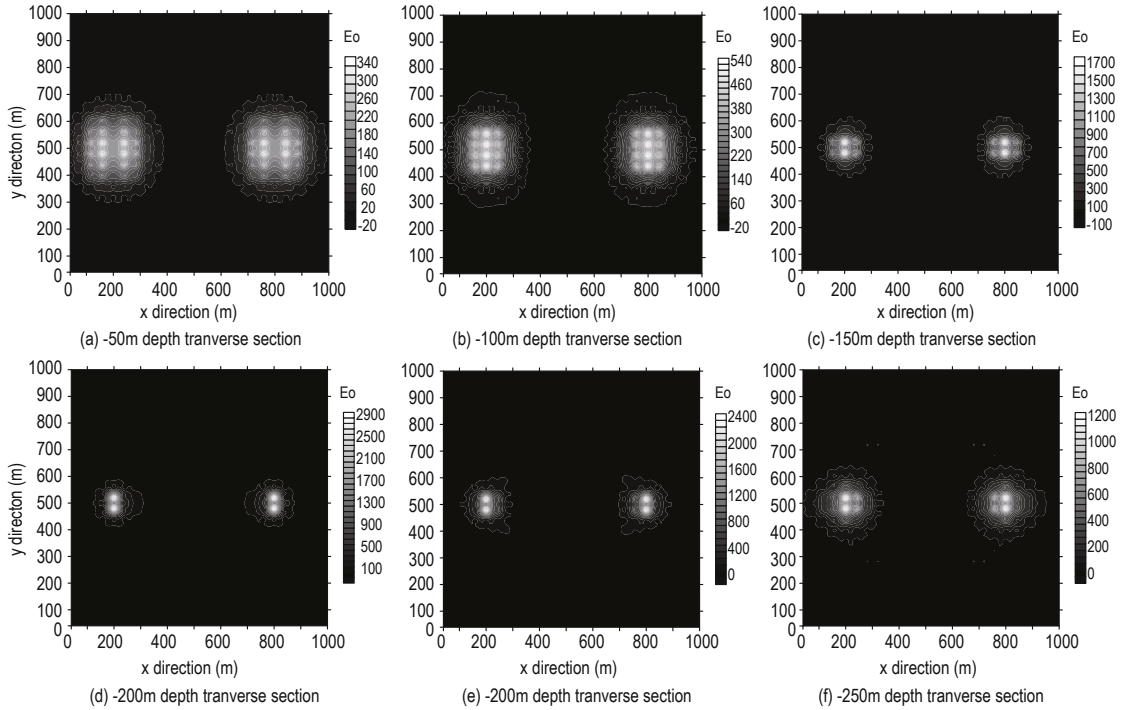

Fig.3 Location of the mass center of the model density anomaly.

Overall, comparing Figures 1d and 1g and Figures 1f and 1i, we may conclude that 3D inversion solutions derived with the extrapolated Tikhonov regularization algorithm in conjunction with the modified depth weighting function based on the gravity gradient eigenvector are more reliable than solutions derived with the Tikhonov regularization algorithm.

Field data

Field data were collected at the Kauring test site (116° 56' 20.52"E, 31° 52' 1.56"S), which is located approximately 115 kilometers east–northeast of the Jandakot Airfield in Perth, Western Australia, and has

been used since 2009 for the testing and calibration of Airborne Gravimetry (AG) and Airborne Gravity Gradiometry (AGG) systems. Fugro Airborne Surveys conducted the airborne gradiometry at the Kauring test site during July 2011 to February 2012, using the FALCON airborne gravity gradiometer (AGG). We performed density inversion using the six measured gravity gradient components in this area. Terrain correction was applied to the gravity gradient data of the survey area, which helps the density inversion of underground anomalies. The six gravity gradient components T_{ee}, T_{nn}, T_{ne}, T_{nd}, T_{ed}, and T_{d} are shown in Figure 4; subscripts e, n, and d correspond to the north-, east-, and down-axis directions of the local geographic coordinates.

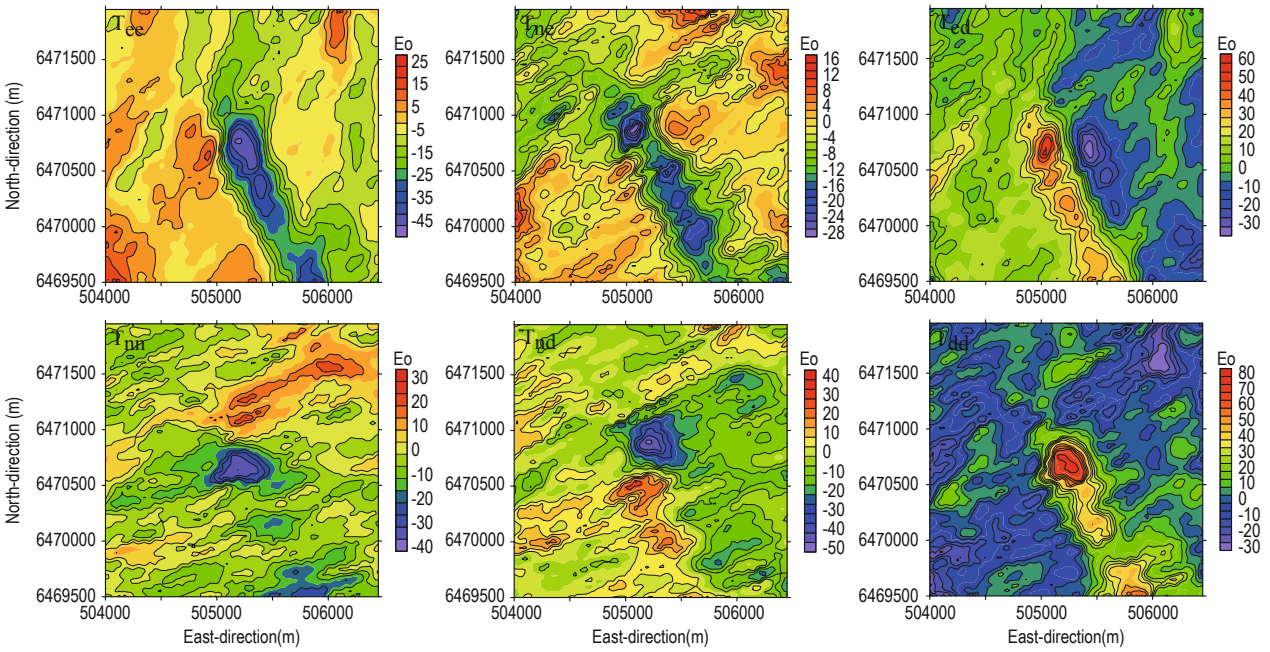

Fig.4 Gravity gradient tensor data at the Kauring test site.

The gravity gradient range chosen for the density inversion is 504 km−506.4 km East and 6469.5 km −6471.9 km North. The spatial dimensions for the density inversion are 2400 m × 2400 m × 1200 m. The dimensions of each prism are 120 m × 120 m × 120 m; thus, there are 4000 prisms. First, we use the modified depth weighting function to locate the mass center of the density anomaly. The results are shown in Figure 5. Three depth transverse sections at −240 m, −360 m, and −480 m are shown and the depth of the mass center of the density anomaly is around −360 m based on the amplitude of the cumulative value. The inversion density vectors of the anomaly are calculated with the extrapolated Tikhonov regularization method in

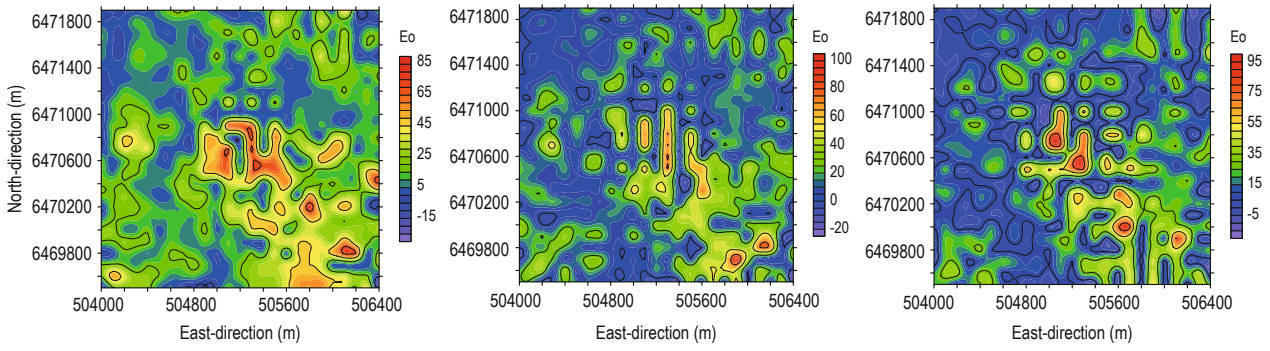

(a) -240 m depth transverse section (b) -360 m depth transverse section (c) -360 m depth transverse section

Fig.5 Location of the mass center of the density anomaly at the Kauring test site.

conjunction with the depth weighting function using the gravity gradient eigenvector. The results are shown in Figure 6. Figures 6b, 6c, and 6d show the −240 m, −360 m, and −480 m depth transverse sections. The distribution of the inversion density is around −360 m in line with the results of the mass center location. The derived anomaly densities range is 0−2.4410 kg/m^3, and the upper limit of the inversion density solutions agrees well with the result (2.4 kg/m^3) of Martinez and Li (2012).

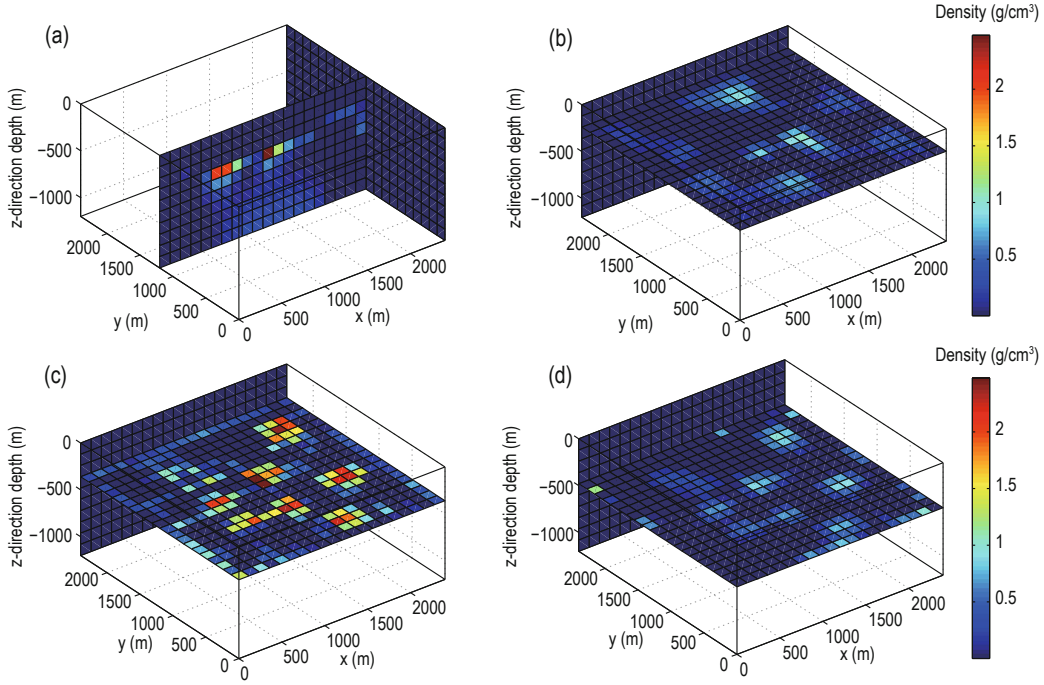

Fig.6 Inversion densities from gravity gradient data at the Kauring test site.
(a) Vertical section y = 1200 m; (b) Transverse section z = −240 m; (c) Transverse section z = −360 m; (d) Transverse section z = −480 m.

Conclusions

We applied the extrapolated Tikhonov regularization and the modified depth weighting function to the 3D density inversion of gravity gradient data. Using model data, we tested the extrapolated Tikhonov regularization algorithm by linearly combining the approximate solutions corresponding to the different regularization parameters of the Tikhonov regularization and minimizing the error between predictions and observations. The proposed algorithm avoids errors owing to the introduction of regularization parameter and improves the robustness of the inversion.

The rapid attenuation of the position function with increasing depth may affect the surface distribution of the inversion results. Hence, we used a modified depth weighting function based on the eigenvector of gravity gradient tensor data to eliminate any undesired effects. The modified depth weighting function is based on the gravity gradient and can be used to accurately detect the mass center of the anomaly. The model data suggested that the depth weighting function improved the resolution in the vertical direction; furthermore, the inversion results for the shallow parts were superior to the results for the deeper sections.

Finally, we conducted 3D density inversion of gravity gradient data from the Kauring test site in Australia and compared the 3D inversion with published results to verify the effectiveness of the proposed method under the conditions of insufficient prior information.

References

Bear, G. W., Al-Shukri, H. J., and Rudman, A. J., 1995, Linear inversion of gravity data for 3-D density distributions: Geophysics, **60**(5), 1354−1364.

Beiki, M., and Pedersen, L. B., 2010, Eigenvector analysis of gravity gradient tensor to locate geologic bodies: Geophysics, **75**(6), 137−149.

Chen, S. H., Zhu, Z. Q., Lu, G. Y., et al., 2013, Inversion of gravity gradient tensor based on preconditioned conjugate gradient: Journal of Central South University(Science and Technology), **44**(2), 619−625.

Commer, M., 2011, Three-dimensional gravity modelling and focusing inversion using rectangular meshes: Geophysical Prospecting, **59**(5), 966−979.

Dransfield, M., 2007, Airborne gravity gradiometry in the search for mineral deposits: Proceedings on Mineral Exploration edited by B. Milkereit, Fifth Decennial International Conference, 341−354

Feng, J., Meng, X. H., Chen, Z. X., et al., 2014, The investigation and application of three-dimensional density interface: Chinese J. Geophys.(in Chinese), **57**(1), 287−294.

Guo, W. B., Zhu, Z. Q., and Lu, G. Y., 2011, Quasi-BP neural network inversion of gravity gradient tensor: Journal of Central South University (Science and Technology), **42**(12), 3797−3803.

Guo, L. H., Meng, X. H., Shi, L., et al., 2009, 3-D correlation imaging for gravity and gravity gradiometry data: Chinese J. Geophys. (in Chinese), **52**(4), 1092−1106.

Hämarik, U., Palm, R., and Raus, T., 2007, Use of extrapolation in regularization methods: Journal of Inverse and Ill-Posed Problems, **15**(3), 277−294.

Hämarik, U., Palm, R., and Raus, T., 2008, Extrapolation of Tikhonov and Lavrentiev regularization methods: 6th International Conference on Inverse Problems in Engineering: Theory and Practice; Journal of Physics: Conference Series, **135**(1), 1−8.

Ke, X. P., Wang, Y., Xu, H. Z., et al., 2009, The three-dimensional crustal structure of the Tibetan plateau from gravity inversion:Progress in Geophysics (in Chinese), **24**(2), 448−455.

Lee, J. B., 2001, FALCON gravity gradiometer technology: Exploration Geophysics, **32**, 247−250.

Li, Y. G., and Oldenburg, D. W., 1996, 3-D inversion of magnetic data: Geophysics, **61**(2), 394−408.

Li, Y. G., and Oldenburg, D. W., 1998, 3-D inversion of gravity data: Geophysics, **63**(1), 109−119.

Li, Y. G., 2001, 3-D inversion of gravity gradiometer data: 71st Ann. Soc. Expl. Geophys. Mtg., Expanded Abstracts,, Expanded Abstracts, 1470−1473.

Liu, Y. P., Wang, Z. W., Du, X. J., et al., 2013, 3D constrained inversion of gravity data based on Extrapolation Tikhonov regularization algorithm: Chinese J.Geophys.(in Chinese), **56**(5), 1650−1659.

Martinez, C., and Li, Y. G., 2012, Understanding gravity gradiometry processing and interpretation through the Kauring test site data: 22nd ASEG International Geophysical Conference and Exhibition, 1−4.

Palm, R., 2010, Numerical comparison of regularization algorithms for solving ill-posed problems: PhD Thesis, University of Tartu.

Rama, P., Rao, K. V., Swamy, I. V., and Radhakrishna Murthy, 1999, Inversion of gravity anomalies of three-dimensional density interfaces: Computers & Geoscience, **25**(8), 887−896.

Pawlowski, B., 1998, Gravity gradiometry in resource exploration: The Leading Edge, **17**, 51−52.

Routh, P. S., Greg, J., Jorgensen, Jerry L. Kisabeth, 2001, Base of the salt imaging using gravity and tensor gravity data: 71st Ann. Soc. Expl. Geophys. Mtg., Expanded Abstracts Expanded Abstracts, 1482−1484. http://library.seg.org/doi/abs/10.1190/1.1816386

Rama, P., Rao, K. V., Swamy, I. V., and Radhakrishna, M., 1999, Inversion of gravity anomalies of three-dimensional density interfaces: Computers & Geoscience, **25**(8), 887−896.

Hämarik, U., PalmR., and Raus, T., 2010, Extrapolation of Tikhonov regularization method, Mathematical Modelling and Analysis, **15**(1), 55−68.

Vasilevsky, A., Droujinine, A., and Evans, R., 2005, Regularized inversion of 3D full tensor gradient (FTG) data for dynamic reservoir monitoring: 75th Ann. Soc. Expl. Geophys. Mtg., Expanded Abstracts, **24**, 700−703.

Wang, Z. W., Xu, S., Liu, Y. P., et al., 2014, Extrapolated Tikhonov method and inversion of 3D density images of gravity data: Applied Geophysics, **11**(2), 139−148.

Wang, H. R., Chen C., and Du, J. S., 2013, 3-D inversion method and application of gravity gradient tensor data: Oil Geophysical Prospecting, **48**(3), 475−481.

Wedge, D., 2013, Mass anomaly depth estimation from full tensor gradient gravity data: Applications of Computer Vision, IEEE workshop, 526−533.

Zhdanov, M.S., Ellis, R.G., Mukherjee,S., et al, 2002, Regularized focusing inversion of 3-D gravity tensor data: 72nd Ann. Soc. Expl. Geophys. Mtg., Expanded Abstracts, 751−754.

Zhdanov, M. S., Robert Ellis, and Souvik Mukherjee, 2004, Three-dimensional regularized focusing inversion of gravity gradient tensor component data: Geophysics, **69**(4), 925−937.

Liu Jin-Zhao received his Ph.D. (2014) in Geodesy and Surveying Engineering from the Institute of Geodesy and Geophysics, China Academy of Science. His main research interests are in airborne gravity gradiometry.